

Dual Stimuli-Responsive Supramolecular Hydrogel Based on Hybrid Inclusion Complex (HIC)

Jianghua Liu, Guosong Chen,* Mingyu Guo, and Ming Jiang*

*The Key Laboratory of Molecular Engineering of Polymers, Ministry of Education, and
Department of Macromolecular Science, Fudan University, 220 Handan Rd., Shanghai 200433, China*

Received June 29, 2010; Revised Manuscript Received September 2, 2010

ABSTRACT: A novel dual-responsive supramolecular hydrogel composed of an azobenzene (AZO) end-functionalized block copolymer PDMA-*b*-PNIPAM (AZO-(PDMA-*b*-PNIPAM)) and β -cyclodextrin-modified CdS quantum dot (β -CD@QD) has been demonstrated. Based on the host–guest inclusion complexation of AZO of the block copolymers and CD cavities on β -CD@QD, they form a hybrid inclusion complex (HIC). The HIC contains a QD as the core and the block copolymer as the shell with the PNIPAM block as the outer layer. Dynamic light scattering (DLS) and UV–vis spectroscopy investigation proved the HIC structure in diluted solution. Hydrogel formed easily upon heating the aqueous solution of HIC at a concentration as low as 7 wt %; as a result of PNIPAM, aggregation occurred above the LCST. The inclusion complex and the domains of the collapsed PNIPAM chains serve as two distinct cross-links and render the hydrogel excellent dual sensitivity to competitive hosts/guests substitution and to temperature variation. Furthermore, rheology results quantitatively exhibit the hydrogel formation mechanism and the sol-to-gel reversibility following the two external stimuli.

Introduction

Macromolecular hydrogels are three-dimensional networks composed of hydrophilic polymeric backbones and cross-link regions, enabling it to swell a large amount of water. Recently, the stimuli-responsive gel/sol transitions of the hydrogels induced extensive research interest. The stimuli scope includes pH,¹ temperature, redox, light,² magnetic fields, or chemical entities.³ Such hydrogels as “smart” soft materials have been found promising in bioapplications^{4,5} because they could sense environmental changes and self-induce structural transformations.^{6–12} In the past couple of years, introducing reversible noncovalent bonds as cross-linkers made significant contributions to the research of environmental responsive behavior of hydrogels, especially for redox¹³ and pH changes.¹⁴

Obviously, more stimuli responses would generate more flexibility to further applications of the hydrogels. Thus, to design and achieve multiresponsiveness within a single piece of soft material is of significance not only to scientific research but also to potential applications. However, hydrogels integrated by independent multiresponsiveness are more challenging than that with only one stimulus because it may require more critical and complicated chemical structures. Lots of single responsiveness hydrogels have been reported while the soft materials with dual or even multiple responsive behavior are rare. So far, block copolymer strategy is the most popular and efficient way to achieve multiresponsiveness. However, if one only relies on block copolymer structures to achieve independent dual responsiveness, a synthetic triblock copolymer is required in which two blocks are for the dual responsiveness and one block serves as the hydrogel backbone. Until now, hydrogels with dual and independent responsiveness are still limited in the literature. For example, poly-(2-vinylpyridine)-*block*-poly(ethylene oxide)-*block*-poly(glycidyl

methyl ether-*co*-ethyl glycidyl ether) (P2VP-*b*-PEO-*b*-P(GME-*co*-EGE)) triblock terpolymer prepared by anionic polymerization exhibited thermo- and pH-reversible gel formation in aqueous solutions.¹⁴ β -CD is a cyclic oligosaccharide composed of seven glucopyranose units with a hydrophilic external cavity and hydrophobic internal surface. This particular structure allows it to selectively accommodate a variety of molecules as guests (e.g., adamantane, azobenzene, and other suitable molecules). Recently, inclusion complexation between β -cyclodextrin (β -CD) and guest molecules has been employed as an alternative non-covalent bond to prepare hybrid system anchoring inorganic components to polymer chains. In fact, embedding inorganic nanoparticles or nanosheets into polymer matrices has proved to be an effective method of enhancing the functionality of the material.¹⁵ Such hybrid hydrogels are reported to have useful mechanical, optical, or magnetic properties.^{16,17} Harada et al.¹⁸ prepared hybrid hydrogel through CD-functionalized carbon nanotube. Our group introduced β -CD-modified SiO₂ nanoparticle as a *supra-cross-link* to poly(ethylene glycol) (PEG), which promotes the formation of hybrid hydrogel.¹⁹ In the study, the interaction of silica nanoparticle with PEG was based on the inclusion complexation between β -CD and adamantane, which is specific enough to have a well-organized hybrid nanocomposition. In addition, there are several other kinds of hydrogels that have been achieved via inclusion complexation of CDs with guests, including thermo- or pH-dissociative α -CD/PEG pseudorotaxanes^{20,21} and photoresponsive hydrogel of modified β -CD with azobenzene grafted polymer reported by the Stoddart²² group.

Quantum dots (QDs) are a large family of inorganic nanocrystals with quantum-confined physical properties, which have important advantages including narrow and size-dependent emission spectra, multicolor excitation, and excellent photostability against photobleaching.^{23,24} The most commonly used QDs are of the cadmium chalcogenide group due to ease of synthesis and handling.^{25,26} The integration of QDs with different

*Corresponding authors: e-mail guosong@fudan.edu.cn (G.C.), mjiang@fudan.edu.cn (M.J.); Fax +86 21-65643919.

materials will provide a new generation of fluorescence markers for biological assay. As a typical kind of soft material, hydrogels can provide an ideal environment hosting a variety of functional molecules and nanoparticles, including QDs.

In this study of dual-responsive hybrid hydrogels, the key point is the combination of the two independent cross-links. A new type of hybrid inclusion complex (HIC) is constructed by connecting QD with diblock copolymer chains, one block of which has thermo-responsiveness. The HIC solution can easily be converted to the designed hybrid hydrogels upon heating. This tailor-made design renders the hydrogel not only thermo-reversibility but also responses to supramolecular substitutions. Furthermore, the effectiveness of this HIC structure brought down the critical hydrogel concentration to be 7 wt %, a rather low concentration among that of some reported stimuli-responsive supramolecular polymeric hydrogels.

Results and Discussion

Design of HIC and Synthesis of AZO-(PDMA-*b*-PNIPAM). We aimed to design a star-shaped hybrid inclusion complex

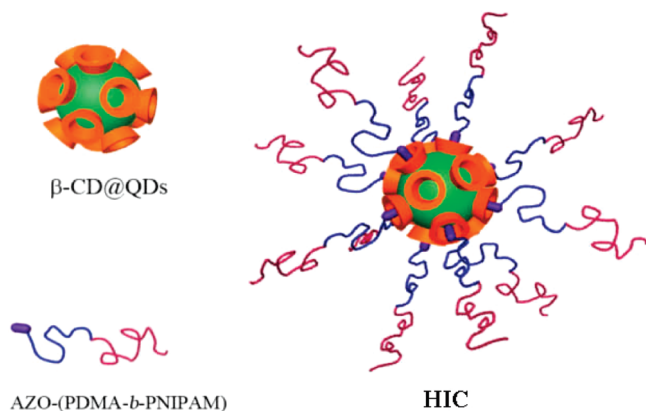


Figure 1. Schematic structures of β -CD@QD, AZO-(PDMA-*b*-PNIPAM), and the hybrid inclusion complex (HIC).

(HIC) rather than triblock copolymer to construct a novel supramolecular hydrogel with dual responsiveness (Figure 1). To this end, a β -CD-covered CdS quantum dot (β -CD@QD) was employed as the core of HIC. In the HIC, the core is connected to the block copolymer chains of AZO-(PDMA-*b*-PNIPAM), by means of the host-guest inclusion complexation between the β -CD on the surface of β -CD@QD and the azobenzene (AZO) group of the copolymer (Figure 1). Therefore, in the HIC, surrounding the core, there are two polymer layers, i.e., the inner layer of poly(*N,N*-dimethylacrylamide) (PDMA), which always keeps solvated in water, and the outer layer of PNIPAM, which turns insoluble to form interchain aggregates when temperature increases to above the LCST of PNIPAM. Thus, the domains of the collapsed PNIPAM chains would connect HIC to form the network, i.e., hydrogel. Obviously, this HIC-based hydrogel possesses two different physical cross-links, i.e., β -CD@QD connecting polymer chains via supramolecular interactions and the temperature-sensitive PNIPAM domains. The presence of the two independent cross-links is the basis for realizing dual-responsive properties of the hydrogels.

To synthesize AZO-(PDMA-*b*-PNIPAM) block copolymer, we designed and prepared a novel AZO-functionalized chain transfer agent (AZO-CTA), which is shown in Scheme 1. AZO-CTA was prepared by a conventional *N,N'*-dicyclohexylcarbodiimide (DCC)-mediated esterification of 4-phenylazophenol with *S*-ethyl-*S'*-(α,α' -dimethyl- α'' -acetic acid)trithiocarbonate (Scheme 1). Then, AZO-CTA was applied for initiating the polymerization of DMA. The polymerization was stopped at about 90% monomer consumption, and subsequently, the obtained homopolymer was further utilized as macroAZO-CTA for the polymerization of NIPAM to yield AZO-(PDMA-*b*-PNIPAM) (Scheme 1). Six AZO-(PDMA-*b*-PNIPAM) samples with different degrees of polymerization (DP) and different DP ratios of PDMA to PNIPAM were prepared as shown Table 1. The theoretical DP and experimental DP of the six polymers are listed. All of the obtained

Scheme 1. Synthetic Route of AZO-(PDMA-*b*-PNIPAM) Block Copolymer

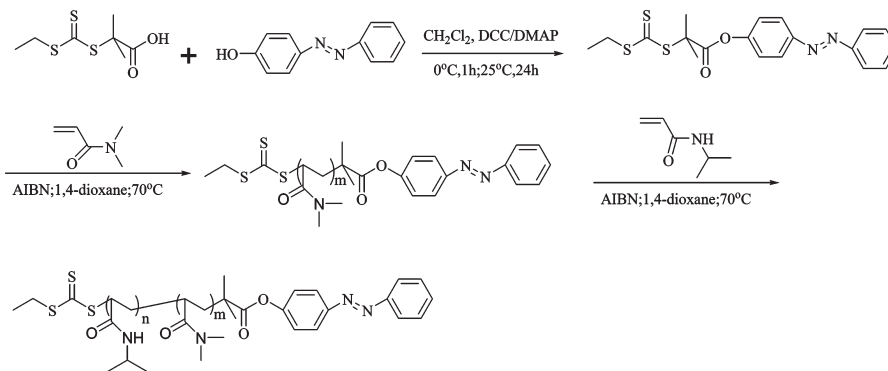


Table 1. AZO-(PDMA-*b*-PNIPAM) Block Copolymers Synthesized in This Study

AZO-(PDMA _{<i>m</i>} - <i>b</i> -PNIPAM _{<i>n</i>})	DP(theoretical) ^a		DP(experimental) ^b		PDI _{CTA} ^c	PDI ^d
	<i>m</i>	<i>n</i>	<i>m</i>	<i>n</i>		
AZO-I-1	100	80	109	89	1.13	1.13
AZO-I-2	100	120	104	138	1.09	1.19
AZO-I-3	100	200	122	223	1.09	1.21
AZO-II-1	200	80	219	84	1.14	1.16
AZO-II-2	200	120	230	133	1.15	1.20
AZO-III-2	400	120	307	127	1.14	1.15

^a Indicative theoretical DP of each block. ^b Determined by ¹H NMR. ^c PDI_{CTA} of macroAZO-CTA, determined by GPC results. ^d PDI of AZO-(PDMA-*b*-PNIPAM), determined by GPC results.

polymers show a well-defined structure, exhibiting a relatively narrow molecular weight distribution indicated by the polydispersity indexes (PDI) below 1.20 determined by GPC (Figure 2). The block ratios of AZO-(PDMA-*b*-PNIPAM) were calculated from the characteristic peak area of methyl groups on DMA and NIPAM in the ^1H NMR spectrum, while DPs were from the ratio of them to that of AZO. Only AZO-I-2 was employed to hydrogel study in details, while the others were used to optimize the hydrogel formation conditions.

Thermo-Responsive Micellization of AZO-(PDMA-*b*-PNIPAM). It is well-known that PNIPAM is soluble in water at room temperature but undergoes a phase separation at its lower critical solution temperature (LCST, commonly $32\text{ }^\circ\text{C}$)²⁷ This thermo-responsive behavior of AZO-I-2 was monitored by dynamic light scattering (DLS). The hydrodynamic radius of AZO-I-2 in solution (1 mg/mL), as expected, from around 5 nm of individual polymer coils at low temperature, starts increasing when temperature increases to $32\text{ }^\circ\text{C}$. Then the size dramatically goes up to the maximum of 38 nm at $36\text{ }^\circ\text{C}$. This indicates the formation of micelles with a hydrophobic PNIPAM core and a hydrophilic PDMA shell. When the temperature increases further, the radius of the micelles begins to decrease from 38 to 23 nm, which is attributed to further dehydration of the PNIPAM blocks.^{28,29} The micelle structure has been observed by TEM (Figure 3B),

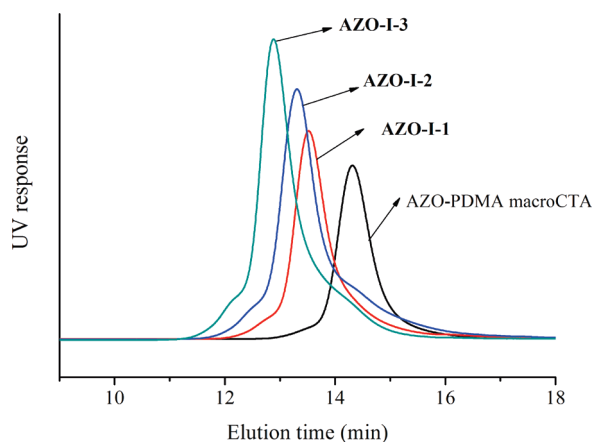


Figure 2. Representative molecular weight distribution of macroAZO-CTA and the corresponding AZO-(PDMA-*b*-PNIPAM) block copolymers (AZO-I-1, AZO-I-2, and AZO-I-3). Eluent: DMF with LiBr (0.5 mg/mL).

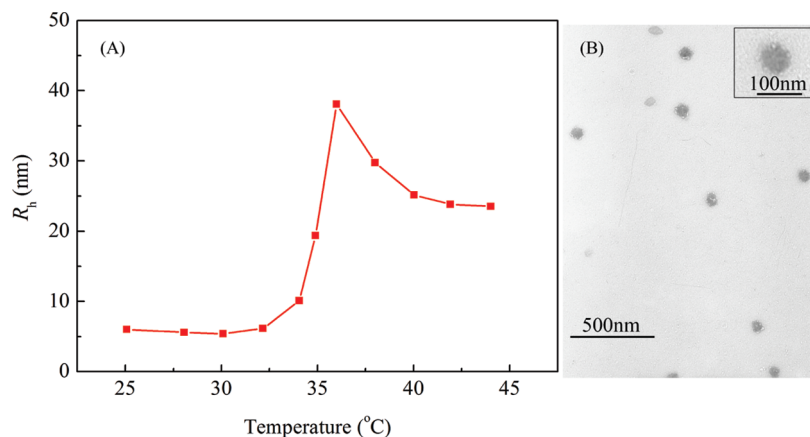


Figure 3. Hydrodynamic radius (R_h) for block copolymer AZO-I-2 in aqueous solution (A) and TEM image of micelles formed by aggregation of PNIPAM blocks above LCST (B). Inset: a typical micelle formed by AZO-I-2.

showing that the micelles are spherical with a radius ranging from 25 to 30 nm, which is consistent with the DLS results.

Inclusion Complexation of AZO-(PDMA-*b*-PNIPAM) with β -CD. The AZO-(PDMA-*b*-PNIPAM) contains AZO end which may act as a guest to form inclusion complexes with β -CD in aqueous solution. Formation of the inclusion complexes of AZO-(PDMA-*b*-PNIPAM) block copolymer with free β -CD was proved by UV-vis spectra. The UV-vis spectra of AZO-I-2 solution alone, and its mixture with different amount of β -CD after ultrasonic treatment for 1 h, are shown in Figure 4. The peaks at 312 and 424 nm are the characteristic absorption peaks of AZO units. The absorption of AZO units at 312 nm gradually decreases while that around 424 nm increases gradually, accompanying a hypsochromic shift (about 15 nm) as the molar ratio of CD to AZO units increases from 0.5 to 80. This is attributed to the high hydrophobicity and high electron density inside CD cavities as a result of CD accommodating AZO units.³⁰ The result implies that, being attached onto the long block copolymer chain, the AZO group still keeps its ability to form inclusion complex with β -CD.

HIC Formation and Characterization. As the core of HIC, β -CD@QDs was prepared according to the reported literature.³¹ The organic content (β -CD content) of β -CD@QDs was found to be 48%, as the weight loss from 250 to $450\text{ }^\circ\text{C}$ measured by thermogravimetry analysis (TGA) (Figure 5). Considering the diameter of β -CD@QDs observed under HR-TEM

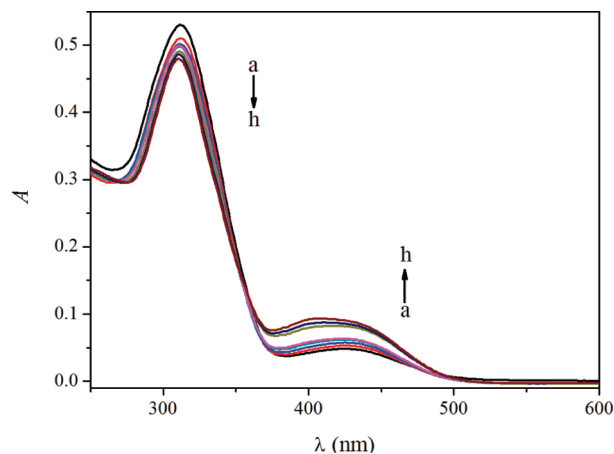


Figure 4. UV-vis spectra of AZO-I-2 block copolymer ($2.0 \times 10^{-5}\text{ mol dm}^{-3}$) in the presence of β -CD ($0, 1.0, 2.0, 10, 20, 40, 60,$ and $80 \times 10^{-5}\text{ mol dm}^{-3}$ from a to h) after ultrasonic treatment for 1 h.

being around 4 nm (Figure S4), the approximate number of β -CD on QD surface was calculated as 22, assuming the surface coverage of β -CD was 80%.³¹ β -CD@QDs and block copolymer AZO-I-2 were mixed in a diluted aqueous solution with molar ratio of β -CD to AZO as 1.5:1. After sonication, the uncomplexed β -CD@QD and/or AZO-I-2 were removed by dialysis (5×10^4 molecular weight cutoff). The obtained HIC was further concentrated and dried by lyophilization and characterized by TGA (Figure 5). The organic content of HIC was found to be 89.8%; thus, each HIC was composed of a β -CD@QD core and block copolymer chains which occupied 63% of CD cavities on the QD surface (calculation method: see Supporting Information).

To achieve the desired hydrogel structure, the thermoaggregation of PNIPAM on HIC should be independent of inclusion complexation. Thus, the temperature-induced phase transition of the HIC at a low concentration of 1 mg/mL (prepared by AZO-I-2 with the molar ratio of β -CD to AZO is 1.5) was investigated by DLS (Figure 6a). A similar size variation as to that of AZO-I-2 solution alone was observed as the temperature increased. Below the LCST of PNIPAM, the hydrodynamic radius of HIC is 8 nm, higher than AZO-I-2 alone in solution (5 nm, in Figure 3a), because the HIC contains a core of quantum dots with a 4 nm diameter. As the temperature increases to LCST, the radius dramatically increases to 35 nm because of the contraction of the PNIPAM chains, which then induces aggregation of the HIC particles. The formed aggregates disperse stably in water due to the low concentration. When the temperature increases further, the radius decreases to about 20 nm because of the further dehydration of the collapsed PNIPAM chains.³² A remarkable feature of the aggregates shown in TEM image is that they do not have a smooth outline, as

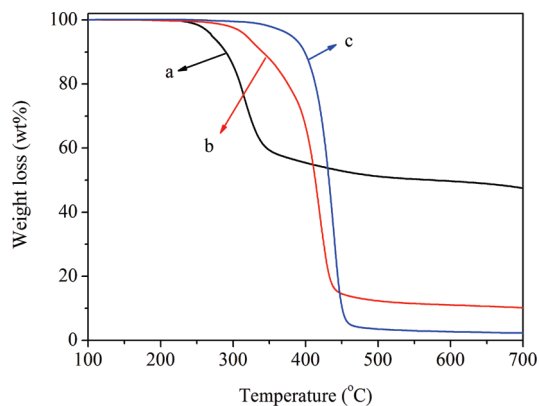


Figure 5. TGA curves of β -CD@QDs (a), HIC (b), and AZO-I-2 (c).

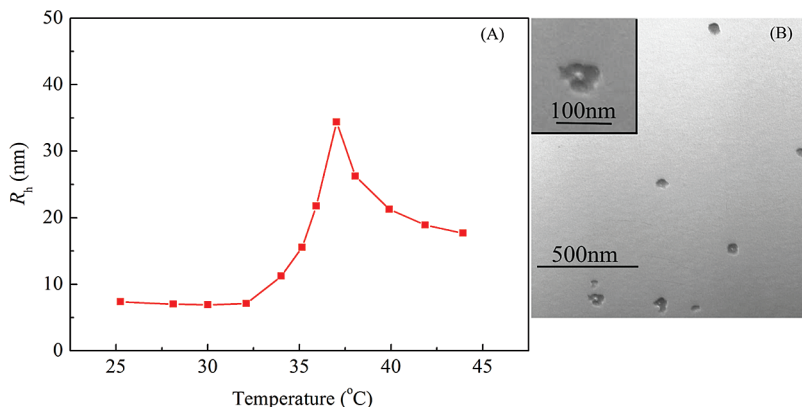


Figure 6. Hydrodynamic radius (R_h) for HIC in aqueous solution (A) and TEM image of HIC in diluted solution above LCST (B).

they are composed of several smaller particles (inset in Figure 6B). This confirmed the formation mechanism we just addressed.

Formation, Photoluminance, and Rheology Study of Supramolecular Hydrogel. In this study, the HIC was used as building blocks to construct hydrogels. In our simple test tube inversion observation of the HIC solutions with a series of concentration from 7 to 25 wt % (weight ratio, the same below), we found that the yellow fluidic, homogeneous solutions can be converted to slightly turbid free-standing gels at 40 °C after a few minutes. Obviously, the PNIPAM chains on the periphery of the HICs collapsed and combined together from different HICs. However, no macroscopic precipitate was formed as the PDMA chains kept solvated. Therefore, hydrogel formed, which is featured by two different cross-links: The first is β -CD@QDs, which connect the network-forming chains of the block copolymer by supramolecular interactions, and the second is the collapsed PNIPAM domains, which link HICs.

The formation of the hydrogel was further monitored by viscosity–temperature measurements on ARES rheometer for concentrations of 12, 15, and 25 wt %. We found the minimum concentration of HIC to form hydrogel after heating is as low as 7 wt %, while the same block copolymer alone without β -CD@QD cannot form hydrogel even when the concentration reached up to 25 wt %. As shown in Figure 7, the viscosity for block copolymer AZO-I-2 solution with 12 wt % varied little with increasing temperature from 30 to 45 °C, while an abrupt viscosity enhancement for its HIC at the same concentration was observed from 35 to 40 °C (Figure 7b), above the LCST of PNIPAM block, indicating the onset of network formation. Subsequently, the viscosity for HIC was

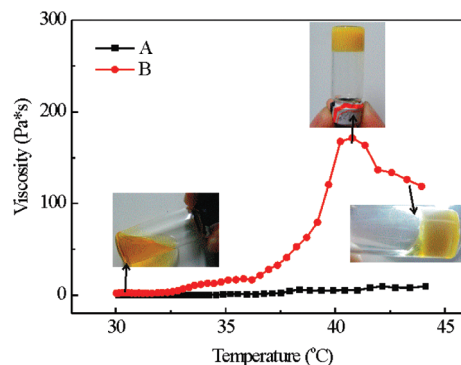


Figure 7. Temperature dependence of viscosity of (A) block copolymer AZO-I-2 solution (12 wt %) and (B) the HIC (12 wt %). The digital photos show the corresponding appearance.

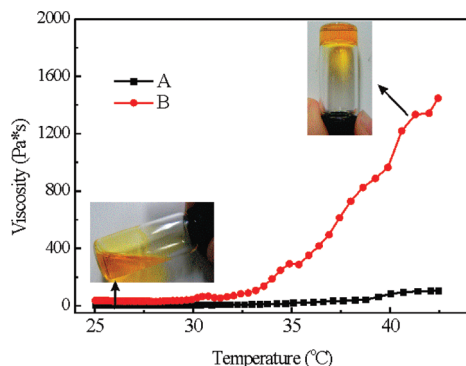


Figure 8. Temperature dependence of viscosity of (A) block copolymer AZO-I-2 solution (25 wt %) and (B) the HIC (25 wt %). Digital photos show the corresponding appearance.

moderately decreasing when the temperature was further increased above 40 °C.

We also found that when the temperature was further increased, or the gel was standing at 40 °C even longer, the hydrogel shrank a little and a thin and transparent layer of water appeared on the surface of the hydrogel. This phenomenon was not hard to understand by considering the previously observed collapse of micelles in diluted solution (Figures 3 and 6), caused by dehydration of the NIPAM blocks. It is worth mentioning that we also observed the shrinking of hydrogel and small amount of water on the parallel-plate surface of rheometer at the end of the experiment.

Figure 8 shows the viscosity variation with temperature for the solutions of AZO-I-2 and its HIC with a concentration as high as 25 wt %. Over the temperature range from 25 to 45 °C, the viscosity of AZO-I-2 solution varied little, similar to that at a lower concentration (Figure 7A), while that of the HIC solution was continuously increasing, obviously different from that of the same HIC at the concentration of 12 wt % (Figure 7). At 40 °C, the viscosity of the 25 wt % solution of HIC reached about 10^3 Pa s, while it was only 180 Pa s for the 12 wt % solution. In fact, the hydrogel formed at 25 wt % was always transparent upon heating to 40 °C and became only slightly turbid after heated to 55 °C. This might be ascribed to that, at higher concentration, the motion of HICs was restricted, so the HICs, particularly the QD cores, did not sufficiently aggregate; instead, they kept homogeneously dispersed.

It is well-known that the sol–gel transition can easily be determined from dynamic rheological data. The temperature at which the elastic modulus G' curve intersects that of the viscous modulus G'' indicates the sol–gel transition point. Figure 9 shows the oscillatory temperature sweep profiles of HIC (formed by AZO-I-2) at concentrations of 12 and 15 wt %. When the temperature was below 32 °C, both HIC solutions exhibit obvious viscoelastic response, where G'' was large than G' , as the HIC was in a liquid state. When the temperature of HIC solution was increased to above 32 °C, both G' and G'' increased. However, the enhancement rate of G' was larger than that of G'' . Then, the sol–gel transition occurs when $G' = G''$ at 40 °C for 12 wt % solution and 41 °C for 15 wt % solution. In addition, from Figure 9, it was also evident that higher concentration of HIC led to higher value of G' and G'' .

Furthermore, the photoluminescence behavior of HIC was measured before and after the hydrogel formation, which is an important property of the soft material we obtained.³³ HIC inherited the trap-state emissions of QDs³¹ (Figure S6) presenting a strong emission around 548 nm. The intensity of

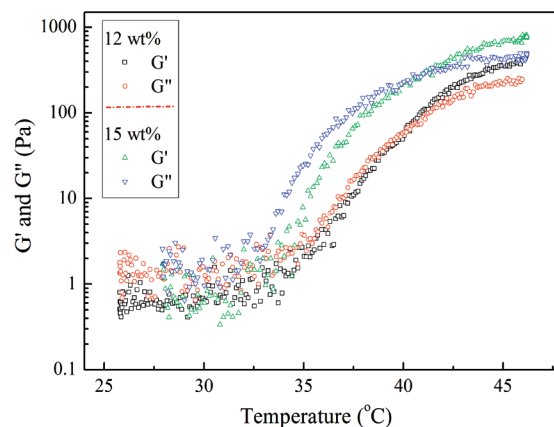


Figure 9. Shear elastic modulus G' and shear viscous modulus G'' for HIC of AZO-I-2 in solution at concentration of 12 and 15 wt % as a function of temperature.

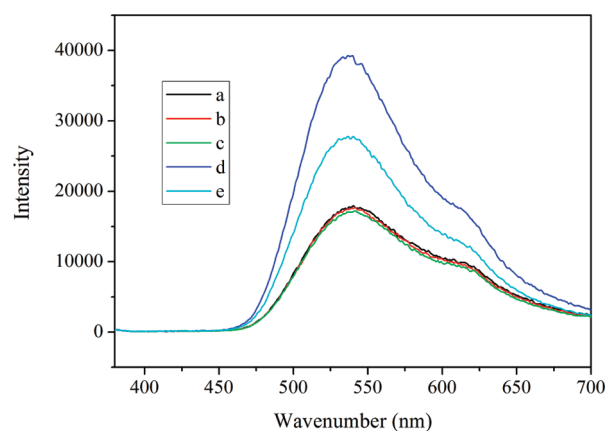


Figure 10. Photoluminescence spectra of HIC at concentration of 15 wt % at different temperatures: (a) 25, (b) 30, (c) 35, (d) 40, and (e) 45 °C (excitation wavelength: 360 nm).

this emission peak did not change much as the temperature variation is between 25 and 35 °C. A sharp increase of photoluminescence intensity was detected as the temperature increased from 35 to 40 °C (Figure 10). At the same temperature range, a dramatic increase of viscosity was observed by rheological study due to the hydrogel formation (Figure 7). It is clear that the higher viscosity of HIC solution confined the movement of QDs leading to a strong enhancement of photoluminescence. After the temperature was further increased from 40 °C, the intensity of the emission decreased, which was probably with the shrinkage of the PNIPAM block.^{34,35}

Reversibility in Gel–Sol Transitions via Thermal Change and Supramolecular Substitution. The supramolecular hydrogel we obtained contains two distinct and independent physical cross-links. Therefore, cleavage of either one of the cross-links would lead to disassociation of the hydrogel. The supramolecular hydrogel formed by HIC of AZO-I-2 at 15 wt % was used to demonstrate the thermo-responsive behavior. We observed that the hydrogel returned to free-flowing, homogeneous solution after cooled to room temperature, with the release of the aggregated PNIPAM chains. This recovered HIC solution returned to hydrogel again as the temperature increased above LCST (Figure S8). This sol-to-gel and gel-to-sol transition was also monitored by the viscosity change with temperature shown in Figure S8, i.e., the viscosity varies from about 10 Pa s at 25 °C to 310 Pa s at 40 °C and then to 10 Pa s at

25 °C again. This thermoreversible sol–gel transition took place fast and could be performed repeatedly for several cycles.

As the host–guest inclusion complexation between β -CD@QDs and AZO units of the block copolymer enables them to serve as cross-link to form network structure, we tried to recognize the gel-to-sol transitions by introducing competitive host and guest into the hydrogels. When water-soluble 1-adamantanamine powder (ADA, 2 equiv to β -CD unites of QDs nanoparticles) was added to the hydrogel as a competitive guest, the gel-to-sol transition was observed within several minutes from top to bottom in the vial. This indicated that the host–guest interaction between β -CDs and AZOs dissociated quickly due to the stronger competitive inclusion complexation of β -CD with ADA. Meanwhile, the hydrogel can be changed to sol by adding α -CD (2 equiv to AZOs) as a competitive host to release the same interaction in HIC. Stronger inclusion complexation of α -CD with AZOs resulted the dissociation of AZOs from β -CDs.³⁶ The resultant disassociated hydrogels (i.e., sol state) by adding competitive guest or host were also characterized by rheology measurements, and the results are shown in Figure 11. It was confirmed that the trend of viscosity variation for the disassociated hydrogels was almost identical to that of AZO-(PDMA-*b*-PNIPAM). Figure 9 shows the images of all transition states. Obviously, the observations that the supramolecular hydrogels were disassociated by adding the competitive guest or host further supported the proposed HIC structure and its gelation mechanism (Scheme 2).

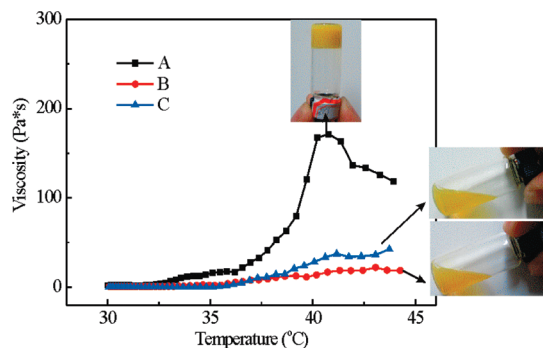
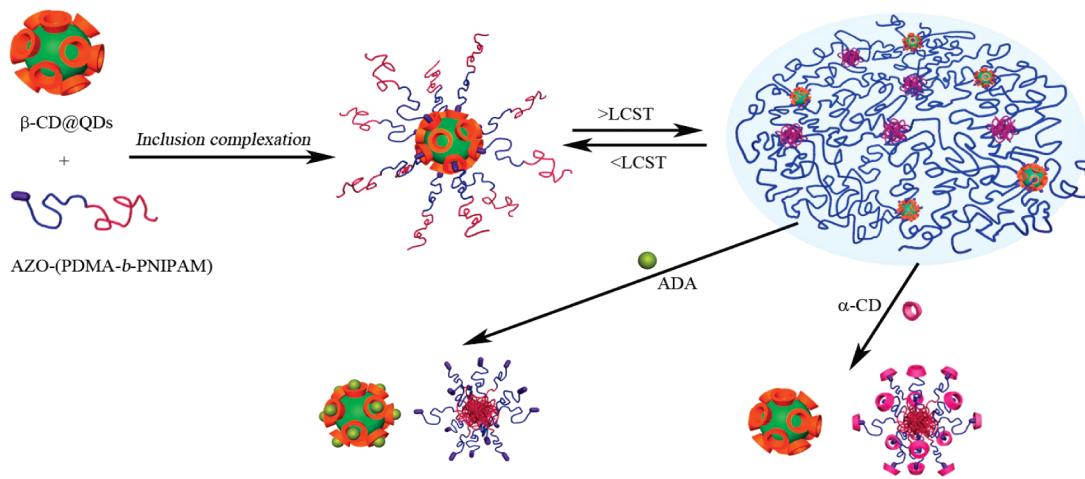


Figure 11. Temperature dependence of viscosity of (A) the HIC solution (12 wt %) and the dissociated hydrogels obtained by adding ADA (B) and α -CD (C). Digital photos show the corresponding appearance.

Other Factors Associated with the Hydrogel Formation. In this system, when total weight (including both AZO-(PDMA-*b*-PNIPAM) block copolymer and QD nanoparticles) is fixed, the molar ratio of β -CD to AZO units of the block copolymers significantly affects the hydrogel formation. We prepared HIC over different β -CD to AZO ratios and calculated the number of block copolymer chains on each QD surface (Table S1). Then we performed the hydrogel formation experiments and investigated the effect of different molar ratios. In two extreme cases, i.e., the molar ratio of β -CD and AZO units being 1:1 and 6:1, neither of them formed hydrogels at concentration of 7 wt %, but hydrogels formed when the concentration is higher than 15 wt %. For the molar ratio 1:1, the concentration of the QD particles is too low to provide enough binding sites. When the ratio is as high as 6:1, the aggregation of PNIPAM cannot lead to the formation of hydrogel network as the concentration of the polymer chains is not enough. We found that the optimum molar ratio of CD to AZO for the gel formation is 1.5:1, in which 63% CDs on each nanoparticle was occupied by block copolymer chains as calculated based on TGA measurements (Supporting Information).

In order to study the influence of degree of polymerization (DP) of PNIPAM and PDMA on gelation, a series of AZO-(PDMA-*b*-PNIPAM) block copolymers with different DPs were prepared (Table 1). For the copolymers AZO-I-1, AZO-I-2, and AZO-I-3 with similar DP of PDMA block ($DP_{PDMA} = 109$), AZO-I-1 with the lowest DP of 89 of PNIPAM block cannot form hydrogel with β -CD@QDs even at a total concentration of 20 wt % with suitable molar ratio of CD to AZO (1.5:1). However, for both AZO-I-2 and AZO-I-3 with higher DPs of PNIPAM being 130 and 223, hydrogel formation was realized at a concentration as low as 7 wt %. A similar difference was also observed for AZO-II-1 and AZO-II-2 with similar DP around 220 for PDMA but different DPs for PNIPAM. Therefore, it is clear that the PNIPAM chains have to be long enough to form the cross-link region above LCST. In addition, for sample AZO-III-2, since the length of PNIPAM is enough, further extension of the length of PDMA does not affect the hydrogel formation. The viscosity variation of HIC at 12 wt % constructed by block copolymers with different PDMA and PNIPAM block length is shown in Figure 12. For copolymers AZO-II-2 and AZO-III-2, which have enough length of PNIPAM, hydrogels can form easily. For AZO-I-2 and AZO-I-3, the longer the PNIPAM block, the lower the aggregation temperature. Meanwhile, for sample AZO-I-3, a similar phenomenon of

Scheme 2. Plausible Formation and Disassociation Mechanisms of the Supramolecular Hydrogel of HIC



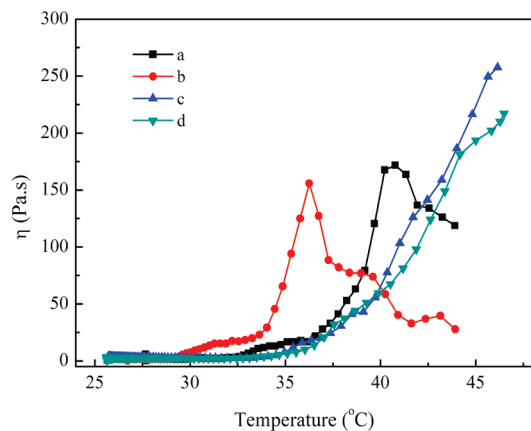


Figure 12. Temperature dependence of viscosity for HIC with 12 wt % concentration constructed by (a) AZO-I-2, (b) AZO-I-3, (c) AZO-II-2, and (d) AZO-III-2.

the reduced viscosity as AZO-I-2 was also observed. This was due to the dehydration of PNIPAM block, and the released water may act as lubricant reducing the apparent viscosity during the stable sweeping measurement. However, for the copolymer with longer PDMA block (AZO-II-2 and AZO-III-2), the viscosity increased continuously after the temperature exceeded the LCST of PNIPAM because of the water absorbance of the longer hydrophilic PDMA, which eliminated the lubricant phenomenon.

Conclusions

We presented supramolecular hydrogels composed of a single supramolecular building block named HIC, which was self-assembled by AZO-(PDMA-*b*-PNIPAM) block copolymer and β -CD@QD via inclusion complexation. Parallel to the thermosensitivity contributed from PNIPAM aggregation, gelation ability of the hybrid core is also effective and tunable by supramolecular substitution. The hydrogel kept the innate fluorescence behavior from quantum dots, which are uniformly distributed in the hydrogel. This property makes the hydrogel a potential candidate for biosensor. The construction of the supramolecular hydrogel via the three-layer HIC may provide a new bottom-up method for designing stimuli-responsive hydrogels, offering great promise of a variety of applications.

Experimental Section

Materials. *N*-Isopropylacrylamide (NIPAM, recrystallized three times from benzene/hexane (65:35 v/v) prior to use) and *N,N*-dimethylacrylamide (DMA, distilled under reduced pressure before polymerization) were purchased from Tokyo Kasei Kagyo Co. 4-Phenylazophenol (97%) was purchased from Alfa Aesar. β -Cyclodextrin (β -CD, CP, recrystallized twice from deionized water) and azodiisobutyronitrile (AIBN, CP, recrystallized from ethanol before use) were supplied by Sinopharm Chemical Reagent Co. Per-7-thio- β -cyclodextrin was prepared according to the literature.^{37,38} Modified CdS quantum dots (β -CD@QD) was prepared by following reported procedure.³¹ Unless specially mentioned, all other chemicals were used as received.

Characterizations. ¹H NMR spectra were recorded with a JEOL ECA-400 spectrometer. Samples were prepared in CDCl₃-*d*. Gel permeation chromatography (GPC) analysis was carried out with a Waters Breeze 1525 GPC analysis system with two PL mix-D column, using DMF with 0.5 M LiBr as eluents at the flow rate of 1 mL/min at 80 °C, PEO calibration kit (purchased from TOSO) as the calibration standard. UV-vis spectra were recorded in a conventional quartz cell (light path 10 mm) on a

Perkin-Elmer Lambda 35 spectrophotometer. Thermogravimetric analysis (TGA) measurements were carried out on a Perkin-Elmer Pyris-1 series thermal analysis system under a flowing nitrogen atmosphere at a scan rate of 20 °C min⁻¹ from 100 to 700 °C. Dynamic light scattering studies of AZO-(PDMA-*b*-PNIPAM) block copolymers and the assembly of AZO-(PDMA-*b*-PNIPAM) and β -CD@QD at concentrations of 1.00 mg/mL in aqueous solution were conducted using ALV/5000E laser light scattering (LLS) spectrometers at scattering angle of 90° and temperature of 25–45 °C. CONTIN analysis was used for the extraction of R_h data. ESI-MS analyses were performed with a Finnigan MAT 95 (San Jose, CA) model LCQ ion-trap mass spectrometer equipped with a Finnigan electrospray ionization (ESI) source and Xcalibur software. The fluorescence spectra of β -CD@QD and HIC at different temperature were measured by FL920 (Edinburg Instruments), equipped with a photomultiplier tube (the samples were excited with UV light of $\lambda = 360$ nm). The morphology of block copolymer and HIC in distilled solution above LCST was analyzed using a Philips EM-430 transmission electron microscope operated at 30 kV. The morphology of β -CD@QD was analyzed using high-resolution TEM on a JEOL JEM2011 electron microscope operating at 200 kV. TEM samples were prepared by spreading a droplet of diluted solution and drying in air under vacuum overnight at 40 °C on copper grids with standard carbon-coated Formvar films on copper grids.

The rheological behavior of the samples was measured by an Advanced Rheology Expanded System (ARES, TA), fitted with a parallel plate (diameter of 50 mm) and circulating environmental system for temperature control. The gap distance between the two parallel plates was fixed at 0.2 mm. The gel formation process was investigated by increasing temperature at a rate of 20 °C/h. The study of the thermoreversibility of samples (Figure S8) was performed by increase and decrease of temperature at a rate of 60 °C/h. Steady rheology measurements were performed by steady-step temperature-ramp test (strain-controlled) at the same shear rate (1 s⁻¹). Dynamic rheology measurements were performed by oscillatory temperature sweeps (stress-controlled) at the oscillation frequency of 1 Hz and the deformation of 0.1.

Synthesis of Azobenzene-Protected RAFT Chain Transfer Agent (AZO-CTA). Trithiocarbonate acid (*S*-ethyl-*S'*-(α,α' -dimethyl- α'' -acetic acid)trithiocarbonate) was prepared as previously reported.³⁹ AZO-protected CTA was prepared by a conventional *N,N'*-dicyclohexylcarbodiimide (DCC)-mediated esterification of 4-phenylazophenol with trithiocarbonate acid precursor as follows: Trithiocarbonate acid (2.24 g, 0.01 mol, 1 equiv) and 4-phenylazophenol (1.98 g, 0.01 mol, 1 equiv) were dissolved in dry dichloromethane (80 mL) in an ice bath, and the mixed solution was purged with nitrogen for 10 min, followed by dropping dichloromethane solution of DCC (4.16 g 0.02 mol, 2 equiv) and 4-(*N,N*-dimethylamino)pyridine (DMAP) (0.245 g, 0.002 mol, 0.2 equiv). After the reaction was carried out at room temperature for 24 h, the resultant mixture was filtered, and the filtrate was concentrated, dissolved in chloroform, and washed with water twice. The organic layer was then dried with MgSO₄, filtered, and concentrated. The residual concentrated solution was chromatographed on silica gel with chloroform as eluent to obtain AZO-CTA. Yield: 3.55 g (84%). ¹H NMR (CDCl₃): $\delta = 1.33$ – 1.38 (t, 3H, CH₃), 1.84 – 1.87 (s, 6H, C(CH₃)₂), 3.31 – 3.38 (q, 2H, CH₂), 7.22 – 7.27 (d, 2H, azobenzene-H _{α}), 7.46 – 7.54 (m, 3H, azobenzene-H _{γ}), 7.87 – 7.96 (m, 4H, azobenzene-H _{β}). ESI-MS: 426.3 [M + Na]⁺.

Typical Synthesis of AZO-PDMA MacroRAFT CTA (MacroAZO-CTA) through RAFT. A typical procedure employed for the preparation of macroAZO-CTA was as follows: AZO-protected CTA (0.2020 g, 0.5 mmol), AIBN (0.01642 g, 0.1 mmol), *N,N*-dimethylacrylamide (4.957 g, 50 mmol), and 5 mL of 1,4-dioxane were added in a 25 mL flask equipped with a magnetic stirring bar. After degassed by freeze-pump-thaw

cycles for three times, the mixed solution was immediately transferred to preheated 70 °C oil bath to initiate the polymerization. After 4 h, the polymerization was quenched by liquid N₂, and the resulting mixture was precipitated in diethyl ether. The precipitate was dissolved in THF and then precipitated again into an excess of diethyl ether. The above dissolution–precipitation cycle was repeated three times. The final product was dried in vacuum, yielding a yellow solid (4.38 g, 87%, $M_{n, GPC} = 4.78 \times 10^3$, $M_{w, GPC}/M_{n, GPC} = 1.09$). The degree of polymerization of the obtained polymer was 104, which was determined based on the integrals of signals corresponding to azobenzene at δ 7.89–7.98 and DMA block at δ 2.76–3.04 according to ¹H NMR. ¹H NMR spectra are shown in Figure S2.

Typical Synthesis of AZO-(PDMA-*b*-PNIPAM) Block Copolymers through RAFT. The average number molecular weight of macroAZO-CTA determined by ¹H NMR is 1.06×10^4 g/mol. The [NIPAM]:[macroAZO-CTA]:[AIBN] ratio was 120:1:0.2, and the detailed synthesis procedure is as follows: a solution of NIPAM (3.21 g, 28.3 mmol), macroAZO-CTA (2.5 g, 2.36×10^{-4} mol), and AIBN (7.75 mg, 4.72×10^{-5} mol) in 12 mL of 1,4-dioxane in a 25 mL flask equipped with a magnetic stirring bar was degassed by freeze–pump–thaw cycles three times. Then the flask was immediately immersed into an oil bath at 70 °C. After stirring for 6 h, the polymerization was terminated by quickly cooled in liquid N₂, and the resultant mixture was precipitated into an excess diethyl ether. The crude product was redissolved in deionized water and dialyzed against deionized water for 7 days with changing water three times per day. The final product was obtained by lyophilization. Yield = 4.8 g, 84%, $M_{n, GPC} = 1.16 \times 10^4$, $M_{w, GPC}/M_{n, GPC} = 1.19$. The degree of polymerization of the PNIPAM block of AZO-(PDMA-*b*-PNIPAM) block copolymer was 138, which was determined based on the integrals of the signals corresponding to azobenzene at δ 7.89–7.98 and NIPAM at δ 1.05–1.25 region in ¹H NMR (Figure S3). Other AZO-(PDMA-*b*-PNIPAM) block copolymers with different degrees of polymerization were prepared through a similar preparation procedure.

Preparation of HIC and Further Formation/Dissociation of the Supramolecular Hydrogels. A representative procedure for HIC and the further supramolecular hydrogels formation is as follows. 16 mg of β -CD@QDs was taken in a 5 mL glass vial containing 0.88 mL of water. After β -CD@QDs was dissolved completely in a few minutes, 104 mg of AZO-(PDMA-*b*-PNIPAM) block copolymer was added to the yellow solution. Here, the molar ratio of β -CD cavities in β -CD@QDs and the azobenzene unit in the block copolymer is ca. 1.5:1. The resultant mixture was stirred for more than 3 days to ensure the inclusion complexation complete, followed by dialysis (molecular weight cutoff of dialysis bag: 5×10^4) and lyophilization. HIC with other CD to AZO ratios were prepared by the same procedure. The hydrogel was formed after heating at 40 °C for 1 h under desired concentration. Other hydrogels were prepared through a similar method.

The general protocol of the dissociation of formed hydrogels by adding competitive host α -cyclodextrin (α -CD) or competitive guest 1-adamantanamine (ADA) is as follows. After hydrogel formation at 40 °C, 10 mg α -CD (2 equiv to azobenzene units of AZO-(PDMA-*b*-PNIPAM) block copolymer) or 2.5 mg ADA (2 equiv to β -CD unites of QDs nanoparticles) was added to the glass vial at 40 °C. Then the hydrogels would exhibit gel–sol transition within a few minutes. When α -CD was added, pH of hydrogel solution was adjusted to pH = 8–10 in order to avoid CD self-association.

Acknowledgment. We thank National Natural Science Foundation of China (NNSFC No. 20834004, 20904005, and 20774021) and Ministry of Science and Technology of China (2009-CB930400) for financial support. G.C. also thanks Heather Edwards from Department of Chemistry, Iowa State University, for her help in the manuscript preparation.

Supporting Information Available: Figures S1–S9 and Table S1. This material is available free of charge via the Internet at <http://pubs.acs.org>.

References and Notes

- (1) (a) He, C.; Kim, S. W.; Lee, D. S. *J. Controlled Release* **2008**, *127*, 189–207. (b) Qiu, Y.; Park, K. *Adv. Drug Delivery Rev.* **2001**, *53*, 321–329.
- (2) Muraoka, T.; Kinbara, K.; Aida, T. *J. Am. Chem. Soc.* **2006**, *128*, 11600–11605.
- (3) Thornton, P. D.; Mart, R. J.; Ulijn, R. V. *Adv. Mater.* **2007**, *19*, 1252–1256.
- (4) Ozay, O.; Ekici, S.; Baran, Y.; Aktas, N.; Sahiner, N. *Water Res.* **2009**, *43*, 4403–4411.
- (5) Jang, J. H.; Jhaveri, S. J.; Rasin, B.; Koh, C.; Ober, C. K.; Thomas, E. L. *Nano Lett.* **2008**, *8*, 1456–1460.
- (6) Qiu, Y.; Park, K. *Adv. Drug Delivery Rev.* **2001**, *53*, 321–339.
- (7) Tsiatsilianis, C. *Soft Matter* **2010**, *6*, 2372–2388.
- (8) Prabaharan, M.; Mano, J. F. *Macromol. Biosci.* **2006**, *6*, 991–1008.
- (9) Sangeetha, N. M.; Maitra, U. *Chem. Soc. Rev.* **2005**, *34*, 821–836.
- (10) Ahn, S. K.; Kasi, R. M.; Kim, S. C.; Sharma, N.; Zhou, Y. X. *Soft Matter* **2008**, *4*, 1151–1157.
- (11) Sutton, S.; Campbell, N. L.; Cooper, A. I.; Kirkland, M.; Frith, W. J.; Adams, D. J. *Langmuir* **2009**, *25*, 10285–10291.
- (12) Gong, C. B.; Wong, K. L.; Lam, M. H. W. *Chem. Mater.* **2008**, *20*, 1353–1358.
- (13) Roberts, M. C.; Hanson, M. C.; Massey, A. P.; Karren, E. A.; Kiser, P. F. *Adv. Mater.* **2007**, *19*, 2503–2507.
- (14) Reinicke, S.; Schmelz, J.; Lapp, A.; Karg, M.; Hellweg, T.; Schmalz, H. *Soft Matter* **2009**, *5*, 2648–2657.
- (15) Zhao, X.; Ding, X.; Deng, Z.; Zheng, Z.; Peng, Y.; Tian, C.; Long, X. *New J. Chem.* **2006**, *30*, 915–920.
- (16) Palui, G.; Nanda, J.; Ray, S.; Banerjee, A. *Chem.—Eur. J.* **2009**, *15*, 6902–6909.
- (17) (a) Haraguchi, K.; Takehisa, T. *Adv. Mater.* **2002**, *14*, 1120–1124. (b) Haraguchi, K.; Li, H.-J. *Macromolecules* **2006**, *39*, 1898–1905.
- (18) Guo, M.; Jiang, M.; Pispas, S.; Yu, W.; Zhou, C. *Macromolecules* **2008**, *41*, 9744–9749.
- (19) Taira, T.; Suzuki, Y.; Osakada, K. *Chem. Commun.* **2009**, 7027–7029.
- (20) Ren, L. X.; He, L. H.; Sun, T. C.; Dong, X.; Chen, Y. M.; Huang, J.; Wang, C. *Macromol. Biosci.* **2009**, *9*, 902–910.
- (21) Vogt, A. P.; Sumerlin, B. S. *Soft Matter* **2009**, *5*, 2347–2351.
- (22) Zhao, Y. L.; Stoddart, J. F. *Langmuir* **2009**, *25*, 8442–8446.
- (23) Chan, W. C. W.; Maxwell, D. J.; Gao, X.; Bailey, R. E.; Han, M.; Nie, S. *Curr. Opin. Biotechnol.* **2002**, *13*, 40–46.
- (24) Oh, J. K. *J. Mater. Chem., ASAP*.
- (25) Hezinger, A. F. E.; Tessmar, J.; Göpferich, A. *Eur. J. Pharm. Biopharm.* **2008**, *68*, 138–152.
- (26) (a) Murray, C. B.; Norris, D. J.; Bawendi, M. G. *J. Am. Chem. Soc.* **1993**, *115*, 8706–8715. (b) Pathak, S.; Choi, S.-K.; Arnheim, N.; Thompson, M. E. *J. Am. Chem. Soc.* **2001**, *123*, 4103–4104.
- (27) Schild, H. G. *Prog. Polym. Sci.* **1992**, *17*, 163–249.
- (28) Convertine, A. J.; Lokitz, B. S.; Vasileva, Y.; Myrick, L. J.; Scales, C. W.; Lowe, A. B.; McCormick, C. L. *Macromolecules* **2006**, *39*, 1724–1730.
- (29) Magenau, A. J. D.; Martinez-Castro, N.; Savin, D. A.; Storey, R. F. *Macromolecules* **2009**, *42*, 8044–8051.
- (30) Szejtli, J. *Pure. Appl. Chem.* **2004**, *76*, 1825–1845.
- (31) Palaniappan, K.; Hackney, S. A.; Liu, J. *Chem. Commun.* **2004**, 2704–2705.
- (32) Qiu, X.; Kwan, S.; Wu, C. *Macromolecules* **1997**, *30*, 6090–6094.
- (33) Yang, J.; Sena, M. P.; Gao, X. In *Reviews in Fluorescence 2007*; Geddes, C. D., Ed.; Springer Science: Berlin, 2009.
- (34) Li, J.; Hong, X.; Liu, Y.; Li, D.; Wang, Y. W.; Li, J. H.; Bai, Y. B.; Li, T. *J. Adv. Mater.* **2005**, *17*, 163–166.
- (35) Fu, H. K.; Kuo, S. W.; Huang, C. F.; Chang, F. C.; Lin, H. C. *Polymer* **2009**, *50*, 1246–1250.
- (36) Liu, Z.; Jiang, M. *J. Mater. Chem.* **2007**, *17*, 4249–4254.
- (37) Ashton, P. R.; Königer, R.; Stoddart, J. F. *J. Org. Chem.* **1996**, *61*, 903–908.
- (38) Rojas, M. T.; Königer, R.; Stoddart, J. F.; Kaifer, A. E. *J. Am. Chem. Soc.* **1995**, *117*, 336–343.
- (39) Lai, J. T.; Filla, D.; Shea, R. *Macromolecules* **2002**, *35*, 6754–6756.